Theor Chem Acc (2009) 123:383–390
DOI 10.1007/s00214-009-0523-2

REGULAR ARTICLE

Thermodynamic features and environmental effects in a two-states molecular device under strict electrochemical control

Costantino Zazza · Giordano Mancini · Nico Sanna · Massimiliano Aschi

Received: 10 November 2008 / Accepted: 29 January 2009 / Published online: 17 February 2009

Abstract The thermodynamic features of a synthetic molecular thread, recently proposed acting as an electrochemically-driven two-states molecular device, have been systematically investigated by means of nanoseconds time-scale classical molecular dynamics (MD) simulations and basic statistical mechanics relations. Results clearly suggest that the accessible conformational space of such a potential molecular switch shows a strong environmental dependence: the reversible molecular switching mechanism observed in liquid solution is effectively suppressed when the synthetic thread is hypothesized working in vacuo. Such a result has been related to a subtle energetic/entropic balance experienced by the whole system (solute and solvent) during the intramolecular conformational transition of the molecular thread, in presence and in absence of the solvent.

Keywords Molecular machines and devices · Environmental effects

C. Zazza (✉) · G. Mancini · N. Sanna
Supercomputing Centre for University and Research, Caspur, via dei Tizii 6/b, 00185 Rome, Italy
e-mail: costantino.zazza@caspur.it

G. Mancini
CNR-IMIP sezione di Bari, c/o Dipartimento di Chimica, Università di Bari, via Orabona 4, Bari, Italy

M. Aschi (✉)
Dipartimento di Chimica, Ingegneria Chimica e Materiali, Università di L'Aquila, via Vetoio (Coppito 1), 67010 L'Aquila, Italy
e-mail: aschi@caspur.it

1 Introduction

Artificial molecular devices and machines have been representing, in the last decades, a very active and intriguing research area [1–5]. The basic idea behind the design and preparation of a molecular device is the possibility of transforming an external stimulus (e.g., light absorption, chemical reagents, electrochemical reduction) into mechanical work at the nanometer scale. In this respect, novel synthetic supramolecular assembly able to perform specific tasks are emerging, and at the same time, are inspiring the scientific community in the development of a bottom–up nanotechnology for the twenty-first century. To this end, biological systems, e.g., ATP-synthase to myosin, do provide excellent examples of highly efficient natural molecular machines [6, 7]. Unfortunately, molecules are not simple mechanical objects but complex and flexible systems undergoing typical thermal fluctuations. Furthermore, the peculiar feature a molecular machine should possess is linked to the ability of funnelling an ad hoc external stimulus into a reduced number, ideally one, of large-amplitude internal motions (see e.g., the fascinating translational isomerism in catenanes [1–5]). A further difficult aspect is also represented by the not negligible role of the surrounding physical environment, i.e., the solvent, whose effect has repeatedly been emerging in experimental measurements [8–17].[1]

Theoretical and computational scientific approach may provide, in this respect, a reliable tool to the understanding of the dynamical concepts and the basic features of the driving forces, at electronic–atomic level, behind a controllable submolecular motion [18]. In a recent

[1] Several examples of recent molecular devices and machines currently working in different physical environments.

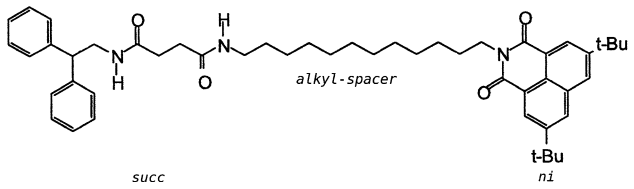

Fig. 1 Molecular structure of the synthetic thread (**1**) recently proposed acting as an electrochemically-driven two-states molecular device [19]. *Succ* stands for succinimide site and *ni* for 3,6-di-*tert*-butyl-1,8-naphthalimide site, respectively

communication [19] we reported a highly efficient and relatively simple electrochemically-driven two-states molecular switch based on a synthetic thread (hereafter termed as **1**, see Fig. 1) for hydrogen-bonded molecular shuttles [20], capable of converting an external perturbation (i.e., oxidation–reduction of 3,6-di-*tert*-butyl-1,8-naphthalimide station, *ni*) into an intramolecular and cyclable elongation-like conformational transition (see Fig. 2). The basic and original idea was to use an essential molecular component of the rotaxanes [20], the linear thread, as a potential molecular machine; the picture emerged from our theoretical and computational investigation indicates that the *succ-[*C_{12} *alkyl-spacer]-ni* thread, in acetonitrile dilute solution (MeCN), changes its free energy minimum conformation as a function of the reduction/oxidation of the *ni*-site. As a matter of fact, as radical anion (reduced species, $\mathbf{1}^{-}$), the synthetic thread basically starting from an elongated conformation F(**1**) undergoes a complete conformational change which: (1) efficiently converts electrochemical energy into mechanical one, (2) brings the *succ* and ni^{-} moieties in close interaction via electrostatic (hydrogen bonding) contacts. This conformational change provides a different and deep free energy minimum basin in which the molecular thread is in a folded conformation, F($\mathbf{1}^{-}$). Furthermore, the process can be reversed, thus the system is reported in its own initial configuration, F(**1**), by oxidation of ni^{-}. This means that a molecular switch able to interchange between these two "conformational" states, i.e., F(**1**) and F($\mathbf{1}^{-}$), in a controllable manner through a selective electrochemical reduction/oxidation of *ni*, has been achieved [19].

In this contribution we extend the results reported in the above communication by explicitly taking into account the effects of the surrounding environment on the thermodynamic features associated to the transformation of the chemical energy into mechanical one. Our strategy is to compare results from classical molecular dynamics (MD) simulations in equilibrium conditions of oxidized and reduced **1** in MeCN, in liquid N–N dimethylformamide (DMF) and in ideal gas-phase conditions.

We wish to remark that the investigation in ideal gas-phase condition, which apparently represents a rather unrealistic condition, may provide interesting mechanical/dynamical features resembling "dry" bidimensional arrays onto a surface [16, 17]. The use of DMF was inspired by experimental data indicating its ability of solvating **1**/$\mathbf{1}^{-}$ [20].

2 Computational details

For a detailed description of the computational setup employed in the present study we invite the interested reader to refer to already cited literature [19]. Herein we only report the basic features and technicalities of our theoretical investigation.

Two classical MD simulations, one for **1** and the other one for $\mathbf{1}^{-}$ species, were carried out at 298 K in MeCN (at its typical liquid density of 782.2 kg/m^3) [21] for 20 ns in a NVT ensemble using an integration step of 2.0 fs with the roto-translational constrain motion applied to the solute [22]. The temperature was kept constant by the isokinetic temperature coupling [23] and all bond lengths were

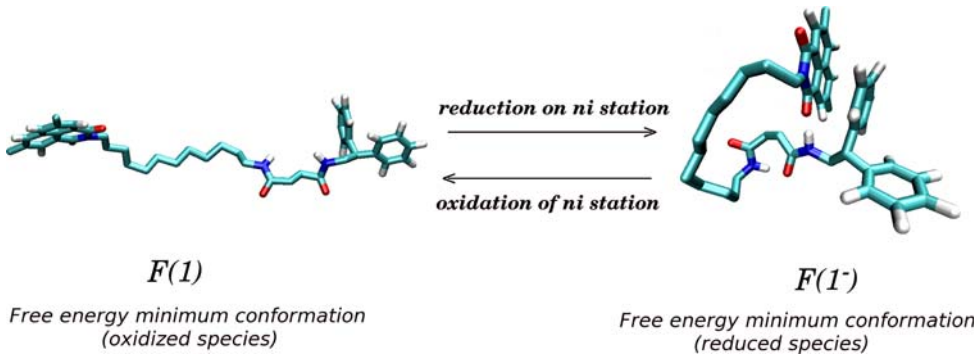

Fig. 2 Schematic view describing the so called elongation-like submolecular motion. When the synthetic thread is in its oxidized species the free energy minimum is basically in an elongated conformation, F(**1**); on the contrary, after the selective reduction of the 3,6-di-*tert*-butyl-1,8-naphthalimide (*ni*) the molecular system is found in a folded conformation, F($\mathbf{1}^{-}$), which is characterized by a strong hydrogen bonding network between the neutral succinimide (*succ*) and radical anion 3,6-di-*tert*-butyl-1,8-naphthalimide (ni^{-})

constrained using LINCS algorithm [24]. Long range electrostatics was computed by the particle mesh Ewald (PME) method [25], with 34 wave vectors in each dimension and a fourth order cubic interpolation. The Gromos force field [26] was used and the atomic point charges of **1** and $\mathbf{1}^-$ were taken from the literature [19]. The same protocol was adopted for simulating **1** and $\mathbf{1}^-$ in liquid N–N DMF [27] and in ideal gas-phase condition.

A preliminary conformational analysis of the trajectories was carried out using essential dynamics (ED) [28] technique, which is based on the construction and diagonalization of the covariance matrix **C** of the positional fluctuations of the all-atoms. This procedure provides a new set of generalized coordinates associated with the eigenvectors of the matrix (i.e., the essential eigenvectors). The value of the corresponding eigenvalues (i.e., the fluctuations along the eigenvectors) allows us to separate the intramolecular large collective essential motions (i.e., the eigenvectors showing the largest eigenvalues) from the remaining small amplitude fluctuations (i.e., mechanically constrained internal motions) [28]. In the light of ED results, *vide infra*, the mechanical behavior of the synthetic thread has been further analyzed following the intramolecular distance (hereafter termed as R_{s-n}) between the geometrical centre of the two end terminals (succinimide and naphthalimide sites, see Fig. 1) along the equilibrated portion of the classical sampling at room temperature. We then evaluated the probability (p_i) of occurrence of a given R^i_{s-n} interval along a pre-defined monodimensional grid. Thus, taking as reference condition (termed as ref) the most recurring interval of inter-terminus R_{s-n} distance (with corresponding p_{ref} and hereafter termed as R_{s-n}*), the Helmholtz free energy ΔA_i associated to the reversible ref $\rightarrow$ i conformational transition may be calculated using the standard formula

$$\Delta A_i = -RT \ln \frac{p_i}{p_{ref}} \quad (1)$$

while the corresponding internal energy variation and entropy change

$$\Delta U_i = U_i - U_{ref} \quad (2)$$

$$\Delta S_i = (\Delta U_i - \Delta A_i)/T \quad (3)$$

may be obtained by averaging the potential energy over the NVT MD frames associated to the i and ref intervals. The errors for the free energy were calculated by dividing the trajectory in two subportions and considering the semi-dispersion of the result (Eq. 1). For the internal energy (Eq. 2) the error was calculated as the mean standard error within the above grid. For the entropy we propagated the above errors according to related Eq. 3.

In analogy with our previous investigation [19] and in order to assess the reliability of the model, we preliminarily calculated the experimentally available ultraviolet (UV) absorption spectrum of the reduced species $\mathbf{1}^-$ in the range 350–470 nm in DMF [20], which corresponds mainly to $^2\pi \rightarrow \pi^*$ electronic excitations of the naphthalimide radical anion [19]. The UV spectrum of $\mathbf{1}^-$ in DMF has been computed applying the recently proposed semi-classical perturbed matrix method (PMM) computational procedure [19, 29–31], in conjunction with TD-PW91/6-311++G(d,p) unperturbed electronic calculations [19] and 20 ns classical MD sampling at room temperature; In this respect, the effects of the classical and fluctuating surrounding environment, at each step of the MD sampling, is modeled as an external and homogeneous perturbing field acting on the unperturbed electronic wavefunctions.

Finally, according to PMM procedure [19, 29–31] in combination with basic statistical mechanics relations we have evaluated the oxidation free energy for removing an electron from the reduced species (radical anion, $\mathbf{1}^-$) confined in its free energy minimum ensemble in gas-phase using the same strategy and the same unperturbed quantum chemical calculations outlined in our previous communication [19].

All the classical MD simulations were carried out using the Gromacs software [32].

3 Results and discussion

3.1 The *succ-[C_{12} alkyl-spacer]-ni* thread in MeCN and DMF

First of all we analyzed the classical MD trajectories in terms of ED technique [28]. Our first aim is to characterize the largest internal fluctuations of the molecular thread and, also, to evaluate the actual convergence of our MD simulations; to this end, the ED analysis was carried out on the most flexible system, i.e., **1** neutral species in MeCN [19]. The spectrum of the all-atoms covariance matrix shows that the conformational fluctuations of **1** may be described by a single eigenvector with a 2.5 nm^2 of eigenvalue versus 0.5 nm^2 of the second one. The projection of the trajectory of **1** in MeCN onto the first essential eigenvector produces the structures depicted in Fig. 3 indicating that the mechanical behavior of the synthetic thread can be also characterized by monitoring the R_{s-n} distance (see Sect. 2). Moreover, we checked the actual convergence of our system by performing ED analysis on the two halves of the **1** trajectory and calculating the overlap of the essential eigenvectors derived from the related ED analysis. The value of 0.8 indicates a very good overlap, providing evidence of the convergence of our simulated system. Therefore, we extended the thermodynamics of **1** in acetonitrile solution whose preliminary results were reported

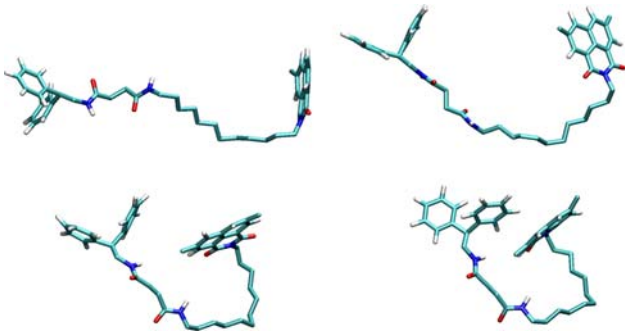

Fig. 3 The *four structures* schematically reported have been obtained by the projection of the classical MD trajectory of the **1** species in acetonitrile solution at 298 K onto the largest internal amplitude fluctuation (first essential eigenvector) of the covariance matrix

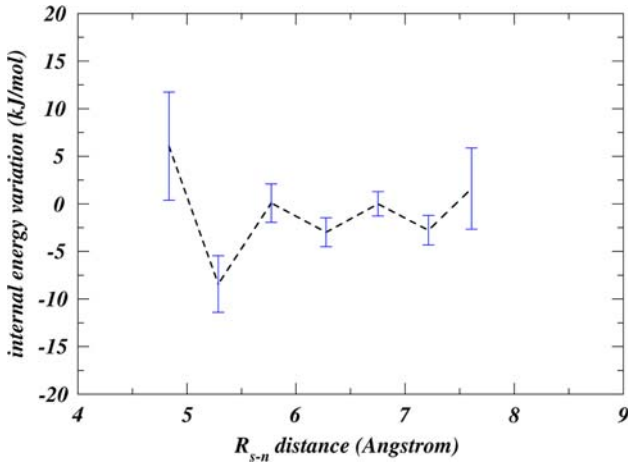

Fig. 4 Internal energy variation (kJ/mol) as a function of $R_{s–n}$ internal coordinate for the synthetic molecular thread (reduced species, $\mathbf{1}^-$) in acetonitrile diluite solution as obtained by means of classical MD sampling at room temperature; the most recurrring interval ($R_{s–n}$* = 6.7 ± 0.2 Å) is taken as reference (i.e., free energy minimum condition, see text)

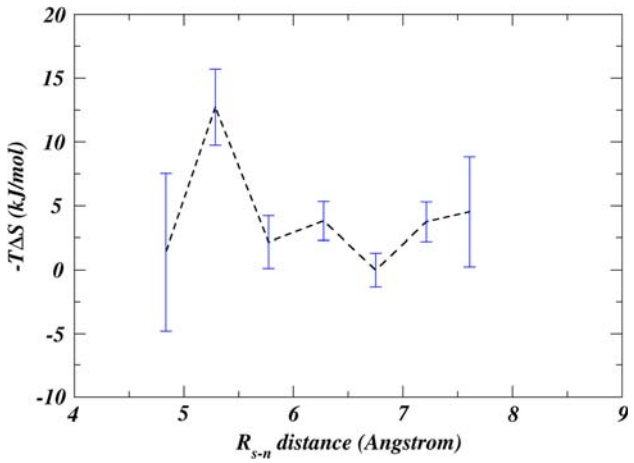

Fig. 5 Entropic factor (kJ/mol) as a function of $R_{s–n}$ internal coordinate for the synthetic molecular thread (reduced species, $\mathbf{1}^-$) in acetonitrile diluite solution as obtained by means of classical MD sampling at room temperature

in our recent communication (see the 298 K Helmholtz free energy profiles depicted in Fig. 3 in Zazza et al. [19]).

The internal energy (ΔU, see Eq. 2) and entropy factor ($-T\Delta S$, see Eq. 3) variation, associated to the equilibrium free energy profile of the reduced species, $\mathbf{1}^-$, in MeCN and reported in Figs. 4 and 5, indicate that $\mathbf{1}^-$ free energy minimum, at about $R_{s–n}$* = 6.7 ± 0.2 Å [19], may be well characterized as a local energetic minimum, therefore showing a not negligible entropic contribution. In fact the lowest internal energy structure, at about $R_{s–n}$ = 5.2 Å, also shows a drastic entropy decrease probably due to the closeness between the radical anion 3,6-di-*tert*-butyl-1,8-naphthalimide and the succinimide moieties, sharply suppressing the internal fluctuations. Such a result suggests that even charged species, as the $\mathbf{1}^-$, is potentially driven in acetonitrile solution both by coulombic and entropic forces. In this respect it should be underlined that both submolecular motions (e.g., the observed translational process of the benzylic amide macrocycle from *succ* to *ni* station [20], and the recently proposed elongation-like conformational change in the *succ-[C_{12} alkyl-spacer]-ni* synthetic thread [19]) result not only as a consequence of the enhancement of the hydrogen-bond-accepting affinity of the *ni*-site as radical anion [33], but also because of entropic factors.

The same quantities are reported in Figs. 6 and 7 for the oxidized species, i.e., **1**. The absolute free energy minimum of **1** lying at $R_{s–n}$* = 18.2 ± 0.2 Å [19], is neither energetically nor entropically disfavoured. As a matter of fact, it does not represent a minimum on the potential energy curve (see Fig. 6) and is not a maximum on the related entropy variation (see Fig. 7). At last, it is also interesting to note that it does exist an entropy maximum, at about $R_{s–n}$ = 11.7 ± 0.2 Å (i.e., partially folded conformations),

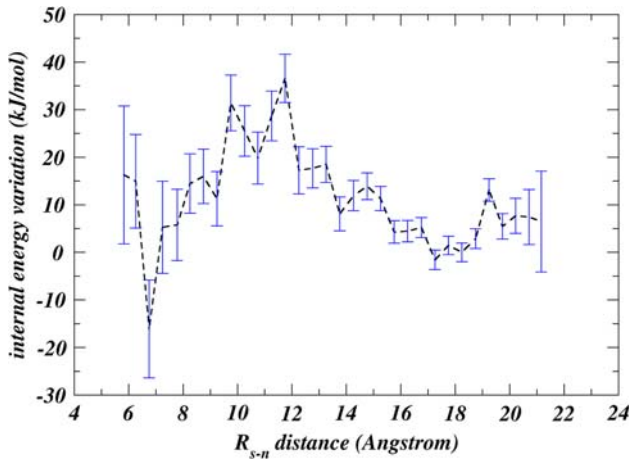

Fig. 6 Internal energy variation (kJ/mol) as a function of $R_{s–n}$ internal coordinate for the synthetic molecular thread (oxidized species, **1**) in acetonitrile diluite solution as obtained by means of classical MD sampling at room temperature; the most recurrring interval ($R_{s–n}$* = 18.2 ± 0.2 Å) is taken as reference

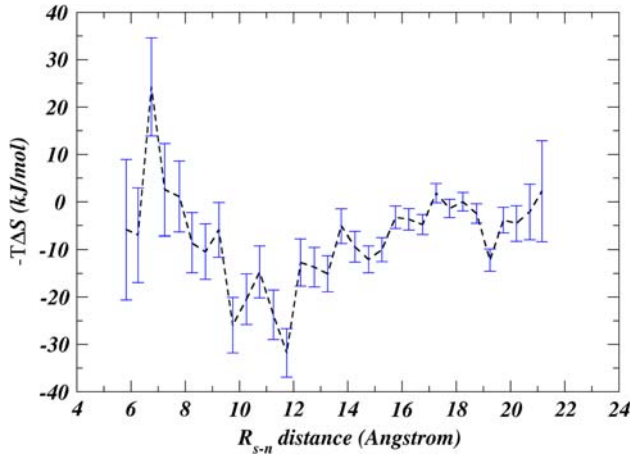

Fig. 7 Entropic factor (kJ/mol) as a function of R_{s-n} internal coordinate for the synthetic molecular thread (oxidized species, **1**) in acetonitrile diluite solution as obtained by means of classical MD sampling at room temperature

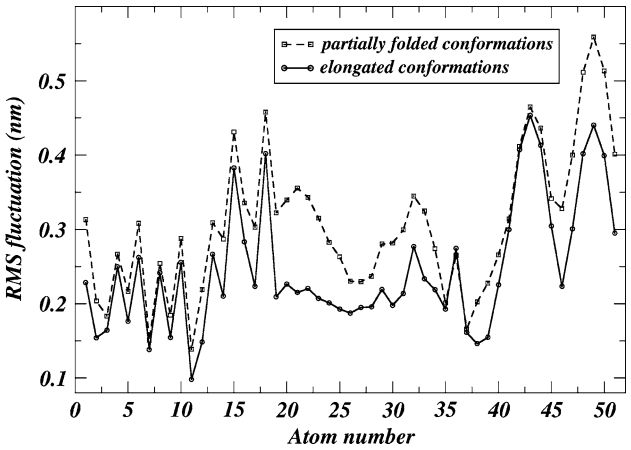

Fig. 8 Root mean squares fluctuations (RMSF, in nm) of the synthetic molecular thread in its oxidized species (**1**); *solid line* (elongated conformations, $R_{s-n}^{*} = 18.2 \pm 0.2$ Å), *dashed line* (partially folded conformations, $R_{s-n} = 11.7 \pm 0.2$ Å)

which is actually counterbalanced by an internal energy increase; on the contrary, an internal energy minimum at $R_{s-n} = 6.7 \pm 0.2$ Å (folded conformations) features a relevant entropy decrease. Furthermore, the presence of a flat region (with R_{s-n} between 8 and 12 Å) in the 298 K Helmholtz free energy profile of **1** species in solution [19] is ascribed to the loss of order in the system over the whole simulated ensemble, thus reflecting an intriguing link between thermodynamic quantities and conformational distributions. More specifically, the thermodynamic analysis reported in Figs. 6 and 7 indicates that, contrary to the situation observed for the folded conformations of **1** at $R_{s-n} = 6.7 \pm 0.2$ Å, the internal energy of the entire system is disfavoured and, most importantly, larger than associated entropy. This implies that the driving force of the conformational relaxation steps in the **1** ensemble upon vertical oxidation, may be identified as energy–entropy compensation effects that dominate the elongation-like process of the thread in acetonitrile solution.

To better figure out the above results we decided to analyze the two "states" on the **1** curve at $R_{s-n}^{*} = 18.2 \pm 0.2$ Å and $R_{s-n} = 11.7 \pm 0.2$ Å. In Fig. 8 we have reported the root mean square fluctuation (RMSF) of the two already quoted states. Our results suggest that the elongated conformations (those confined at $R_{s-n} = 18.2 \pm 0.2$ Å) actually correspond to a 'less fluctuating' state with respect to partially folded ones (see Fig. 8). This may be related to the fact that larger R_{s-n} distances conceivably reduce the conformational repertoire which becomes larger at intermediate distances; In fact, at R_{s-n} lower inter-terminus distance correspond a higher number of **1** accessible conformations by means of thermal fluctuations at 298 K. Additional 3D volumetric density maps of the atomic coordinate at 1.0 Å resolution,

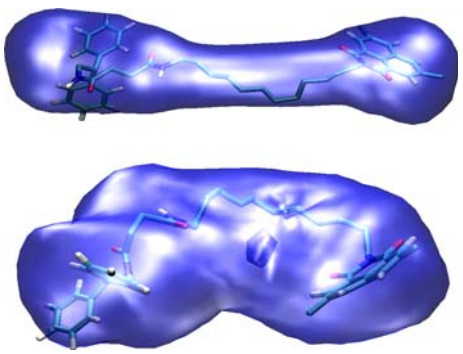

Fig. 9 3D Volumetric density maps for the synthetic molecular thread in its oxidized species (**1**): *upper panel* elongated conformations ($R_{s-n}^{*} = 18.2 \pm 0.2$ Å); *bottom panel* partially folded conformations ($R_{s-n} = 11.7 \pm 0.2$ Å)

calculated by using the MD frames with R_{s-n} distances between 18.2 ± 0.2 and 11.7 ± 0.2 Å (reported in Fig. 9), indicate considerably different conformational flexibility as a function of such a geometrical deformation parameter, thus confirming the trend previously observed in our calculation. Furthermore, in order to evaluate the effect of the solvent we also calculated the solvent accessible surface (SAS) area around the synthetic molecular thread (i.e., the solute). According to the result, reported in Fig. 10 for the above states, the elongated conformations have an uni-modal distribution which provides a SAS expectation value larger than the partially folded state showing a sharp shoulder at almost 9 nm^2. Summarizing, the above data (RMSF, 3D density maps and SAS) may be rationalized invoking an entropy increase of the partially folded conformations (that is $R_{s-n} = 11.7 \pm 0.2$ Å), with respect the elongated ones ($R_{s-n}^{*} = 18.2 \pm 0.2$ Å), which is essentially due to intrinsic (i.e., conformational

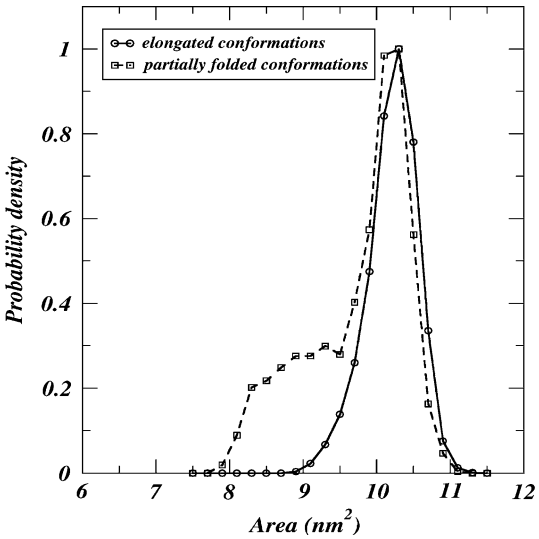

Fig. 10 Solvent accessible surface (SAS) area (nm^2) of the synthetic thread (oxidized species, **1**)/solvent molecules interface; *solid line* (elongated conformations, $R_{s-n}^* = 18.2 \pm 0.2$ Å), *dashed line* (partially folded conformations, $R_{s-n} = 11.7 \pm 0.2$ Å)

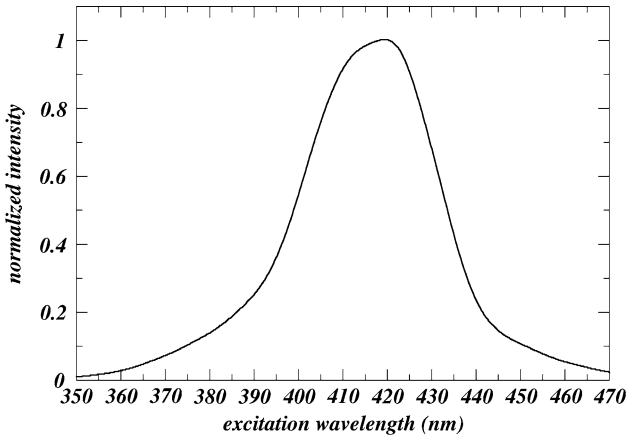

Fig. 11 Calculated, at PMM/PW91/6-311 ++G(d,p) level of computation from 20 ns MD classical simulation in N–N dimethylformamide (DMF) dilute solution, UV spectrum of $\mathbf{1}^-$ molecular system in the range between 350 and 470 nm; The computed maximum shows a λ_{max} at almost 420 nm, while the experimental absorption maximum was found lying at $\lambda_{max} = 422$ nm (see Brouwer et al. [20])

flexibility of the synthetic molecular thread) and environmental (i.e., larger number of free solvent molecules in the partally folded state) effects.

From a computational point of view it is worth noting that classical MD simulations for **1** and $\mathbf{1}^-$, carried out over nanoseconds time-scale in liquid N–N DMF (see Sect. 2), qualitatively provide the same picture as observed for the synthetic thread in MeCN. Unfortunately, since there are not experimental values about the actual redox potential, i.e., reversible work of reduction of the naphthalimide moiety in DMF solution, a comparison between experiments and theory is not, al least at the moment, possible. The only available experimental measurements for $\mathbf{1}^-$ system in DMF are those reported by Brouwer et al. [20] and associated with the UV absorption spectra of the electrochemically generated $\mathbf{1}^-$ species. The absorption maximum characteristic of the naphthalimide radical anion within the synthetic thread was found at 422 nm [20]. Having this in mind, and in analogy with previous findings in MeCN solution [19], we have then decided to theoretically reproduce the UV spectrum of $\mathbf{1}^-$ in DMF, in the range 350–470 nm corresponding to *ni*-site excitations. The calculated UV spectra, which arises from the merging of two $^2\pi \rightarrow \pi^*$ electronic excitations [19], predicts the existence of a single peak with the maximum located at 420 nm and a full width at half maximum (FWHM) of about 32 nm (see Fig. 11). Such a result being consistent with experimental data ($\lambda_{max} = 422$ nm and FWHM of about 30 nm) [20]: (1) points out the ability of PMM methodology in reproducing the spectroscopic properties in molecular systems of high configurational complexity and, most importantly, (2) confirms the reliability and accuracy of the overall computational setup, which supports the presence of an efficient mechanism for converting (reversibly) an electrochemical stimulus into mechanical energy following the oxidation change of the naphthalimide moiety in the *ni-[C_{12} alkyl-spacer]-succ* thread both in MeCN and DMF.

3.2 The *succ-[C_{12} alkyl-spacer]-ni* thread in vacuo

Interestingly, and not unexpectedly, the same procedure carried out in the absence of the solvent produced the result shown in Fig. 12 from which it is clear the absence of any chemical to mechanical work transformation upon oxidation. Indeed, in contrast to the case of **1** and $\mathbf{1}^-$ in MeCN and in liquid N–N DMF, current MD simulations in vacuo clearly indicate that *succ-[C_{12} alkyl-spacer]-ni* synthetic thread, at the equilibrium conditions, appears in both species basically in a closed conformation [$R_{s-n}^*(\mathbf{1}^-) = 5.4$ Å, $R_{s-n}^*(\mathbf{1}) = 6.7$ Å, see Fig. 12]. The folding is induced by intramolecular hydrogen bonding interactions between the lone pairs of the 3,6-di-*tert*-butyl-1,8-naphthalimide oxygen atoms and the hydrogen atoms of the two succinimide amide groups. We remark that both simulations were started from the molecular thread in a fully elongated conformation. Such a result, intuitively explainable on the basis of the 'dielectric' effect of the solvent shielding the coulombic interactions between the two end-terminus (i.e., *succ* and *ni* sites) points out the crucial role of the surrounding physical environment. In turn, this is a successful example of a "wet" stimulative-responsive nanomechanical device exhibiting (energetic/

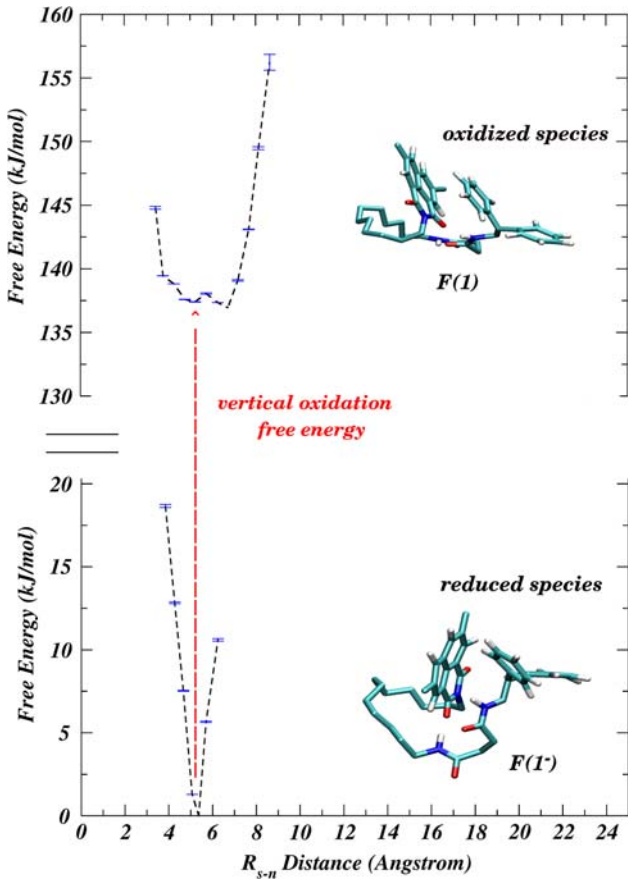

Fig. 12 298 K Helmholtz free energy (at the equilibrium conditions in gas-phase) as a function of R_{s-n} internal coordinate from Eq. 1. As previously reported in acetonitrile dilute solution [19], the *red dashed arrow* indicates the reversible work for removing an electron from the reduced species (i.e., "vertical" oxidation free energy) in gas-phase condition. Structures schematically reported show the representative configurations of the two free energy minima as obtained by classical MD simulations at 298 K in vacuo

entropic balance)-driven switching mechanism with remarkable conformational discrimination. Moreover, the presence of the solvent is found to affect the overall free energy associated with the oxidation of $\mathbf{1}^-$ (ΔA_{redox}); As a matter of fact, the ΔA_{redox} of $\mathbf{1}^-$ in acetonitrile and in gas-phase are estimated to be 124.4 kJ/mol [19] and 136.6 kJ/mol (red dashed arrow in Fig. 12), respectively. This difference in the reversible work for removing an electron from the reduced species confined in its free energy minimum basin is consistent with the conformational (relaxation) free energy following the oxidation of $\mathbf{1}^-$ in solution, that is $\Delta A_{\text{c},\mathbf{1}} = -11.6$ kJ/mol [19].

Consequently, without generalizing the result, the above emerged picture suggests, in nice agreement with experimental statements, [8–17] that a molecular system may act as a molecular device under external influence only in particular environmental conditions. With respect to macroscopic devices and machines, this aspect significantly increases the potentiality of machineries, at the scale of individual molecules, designed for future applications. Therefore, molecular-based machines offer us the possibility to plan and, most importantly to further refine the basic features of nano-technological applications: not only taking into account controllable amplitude fluctuations, but also providing a relatively large field of different miniaturization processes.

4 Conclusions

Classical MD simulations carried out on the synthetic thread **1** in MeCN, in liquid N–N DMF and ideal gas-phase condition, in conjunction with previously published PMM results [19], quantitatively point out the importance of the environmental effects on its performance and, conceivably, on its efficiency as a two-states molecular device. From our investigation it emerges an important and subtle balance between energetic and entropic factors underlying the reversible elongation of $\mathbf{1}^-$ upon selective oxidation of the 3,6-di-*tert*-butyl-1,8-naphthalimide. In particular, the solvent seems to act as a shield modulating the intramolecular coulombic effects but also as a reservoir of entropic forces resulted not negligible in the simulated systems. Furthermore, such an electrochemically-driven two-states molecular switch, being effectively inactive when hypothesized working in vacuo, can be formally characterized as a "wet" molecular device under strict electrochemical control.

Our results, far from being generalized, quantitatively confirm that physico-chemical environmental effects should be seriously taken into account for the design of nanodevices as already emerged in recent experimental works. Other important factors, such as dynamical effects related to the irreversibility of the actual process, should also be investigated and will represent a natural extension of the present investigation currently in progress in our laboratory.

Acknowledgments We gratefully acknowledge Prof. Vincenzo Barone (Chemistry Department, Federico II University, Naples, Italy) and Dr. Andrea Amadei (Science and Chemical Technologies Department, University of Rome "Tor Vergata", Rome, Italy) for stimulating discussions. All the computations were performed at the Supercomputing Centre for University and Research, Caspur (Rome).

References

1. Drexler KE (1986) Nanosystems: molecular machinery, manufacturing and computation. Wiley, New York
2. Balzani V, Credi A, Venturi M (2007) Nanotoday 2:18–25 (and literature therein cited)
3. Jones RAL (2003) Soft machines, nanotechnology and life. Oxford University Press, Oxford
4. Ball P (2000) Nature 406:118–120. doi:10.1038/35018259

5. Credi A (2007) Angew Chem Int Ed 46:5472–5475. doi:10.1002/anie.200700879
6. Fehrst A (1999) Structure and mechanism in protein science: a guide to enzyme catalysis and protein folding. Freeman, New York
7. Squire J, Parry D (2005) Fibrous proteins: muscle and molecular motors, advances in protein chemistry series, vol 71. Academic Press, San Diego
8. Flood AH, Peters AJ, Vignon SA, Steuerman DW, Tseng HR, Kang S, Heath JR, Stoddart JF (2004) Chem Eur J 10:6558–6564
9. Margulies D, Melman G, Shanzer A (2005) Nat Mater 4:768–771
10. Olson DC, Lee YJ, White MS, Kopidakis N, Shaheen SE, Ginley DS, Voigt JA, Hsu JWP (2007) J Phys Chem C 111:16640–16645
11. Steuerman DW, Tseng HR, Peters AJ, Flood AH, Jeppesen JO, Nielsen KA, Stoddart JF, Heath JR (2004) Angew Chem Int Ed 43:6486–6491
12. Stewart DR, Ohlberg DAA, Beck PA, Chen Y, Williams RS, Jeppesen JO, Nielsen KA, Stoddart JF (2004) Nano Lett 4:133–136 (and quoted references therein)
13. Lao C, Li Y, Wong CP, Wang ZL (2007) Nano Lett 7:1323–1328
14. Moorthy JN, Venkatakrishnan P, Huang DF, Chow TJ (2008) Chem Commun 18:2146–2148
15. Badjic JD, Ronconi CM, Stoddart JF, Balzani V, Silvi S, Credi A (2006) J Am Chem Soc 128:1489–1499
16. Jilian H, Tour JM (2003) J Org Chem 68:5091–5103
17. Cecchet F, Rudolf P, Rapino S, Margotti M, Paolucci F, Baggerman J, Brouwer AM, Kay ER, Wong JKY, Leigh DA (2004) J Phys Chem B 108:15192–15199
18. Strajbl M, Shurki A, Warshel A (2003) Proc Natl Acad Sci USA 100:14834–14839. doi:10.1073/pnas.2436328100
19. Zazza C, Amadei A, Sanna N, Aschi M (2008) Chem Commun (Camb) 29:3399–3401. doi:10.1039/b804031a
20. Brouwer AM, Frochot C, Gatti FG, Leigh DA, Mottier L, Paolucci F, Roffia S, Wurphel WH (2001) Science 291:2124–21228. doi:10.1126/science.1057886
21. Grabuleda X, Jaime C, Kollman PA (2000) J Comput Chem 21:901–908. doi:10.1002/1096-987X(20000730)21:10<901::AID-JCC7>3.0.CO;2-F
22. Amadei A, Chillemi G, Ceruso M, Grottesi A, Di Nola A (2000) J Chem Phys 112:9–23. doi:10.1063/1.480557
23. Berendsen HJC, Postma JPM, Van Gunsteren WF, Di Nola A (1994) J Chem Phys 81:3684–3690. doi:10.1063/1.448118
24. Hess B, Bekker H, Berendsen HJC, Frajie JGEM (1997) J Comput Chem 18:1463–1472. doi:10.1002/(SICI)1096-987X(199709)18:12<1463::AID-JCC4>3.0.CO;2-H
25. Darden TA, York DM, Pedersen LG (1993) J Chem Phys 98:10089–10092. doi:10.1063/1.464397
26. Van Gunsteren WF, Billeter SR, Eising AA, Hunemberger PH, Kruger P, Mark AE, Scott VRP, Tironi IG (1996) Biomolecular simulation: the GROMOS96 manual and user guide. vdf Hochschlverlag AG an der ETH Zurich, Zurich
27. Chalaris M, Samios J (2000) J Chem Phys 112:8581–8594. doi:10.1063/1.481460
28. Amadei A, Linsenn ABM, Berendsen HJC (1993) Proteins 17:412–425
29. Zazza C, Amadei A, Sanna N, Grandi A, Chillemi G, Di Nola A, D'Abramo M, Aschi M (2006) Phys Chem Chem Phys 8:1385–1393. doi:10.1039/b515648c
30. Zazza C, Amadei A, Palma A, Sanna N, Tatoli S, Aschi M (2008) J Phys Chem B 112:3184–3192. doi:10.1021/jp0774692
31. Aschi M, Zazza C, Spezia R, Bossa C, Di Nola A, Paci M, Amadei A (2004) J Comput Chem 25:974–984. doi:10.1002/jcc.20029
32. Lindhal E, Hess B, Van der Spoel D (2001) J Mol Model 7:306–317. See also http://www.gromacs.org/
33. Niemz A, Rotello VM (1999) Acc Chem Res 32:44–52. doi:10.1021/ar980046l